Sustainable Biochemicals from Extractives and Pyrolysis Products of *Aesculus chinensis* Bunge Seed Shell

Yiyang Li [a,1,*] Yiran Ma [b,1] Guanyan Li,[c,1] Qian Yang,[a] Tinghe Wang,[a] and Haiping Gu [c]

* *Corresponding author: liyiyang328@163.com*

DOI: 10.15376/biores.22.1.380-405

GRAPHICAL ABSTRACT



Sustainable Biochemicals from Extractives and Pyrolysis Products of *Aesculus chinensis* Bunge Seed Shell

Yiyang Li [a,1,*] Yiran Ma [b,1] Guanyan Li,[c,1] Qian Yang,[a] Tinghe Wang,[a] and Haiping Gu [c]

Forestry waste, which is commonly used as animal feed or burned on-site, holds considerable potential as feedstocks for high-value bioenergy. Hence, their conversion into bioenergy offers a viable pathway to alleviate global energy pressures. *Aesculus chinensis (A. chinensis)* Bunge is a major forest tree species, but its seed shells remain largely underutilized and wasted. This study primarily investigated the bioenergy potential of *A. chinensis* Bunge seed shell waste for satisfying societal energy needs. Extractives were characterized by Fourier-transform infrared spectroscopy (FT–IR) and gas chromatography-mass spectrometry (GC–MS). Thermogravimetric analysis (TGA, 30 to 300 °C at 5 °C/min) was used to characterize the mass-loss stages, and pyrolysis-gas chromatography-mass spectrometry (Py/GC–MS) analyzed the product composition. GC–MS tentatively identified guanethidine, clindamycin, and D-mannose. Py/GC–MS identified 192 compounds, wherein alcohols/phenols and hydrocarbons accounted for 32.2% and 41.0% of the relative peak area, respectively. Organic acids, aldehydes, and ketones were also detected. This study aimed to assess the potential of *A. chinensis* Bunge seed shell waste as a feedstock for both bioenergy and value-added chemicals, using chemical characterization and pyrolysis behavior analysis as the basis for this assessment.

DOI: 10.15376/biores.22.1.380-405

Keywords: Forestry waste valorization; Aesculus chinensis; Seed shell waste; Bioactive extractives; Thermochemical conversion

*Contact information: a: School of Landscape Engineering, Henan Vocational College of Agricultural, Zhengzhou 451450, China; b: School of Life Sciences, Zhengzhou University, Zhengzhou, 450001, China; c: School of Forestry, Henan Agricultural University, Zhengzhou 450000, China; *Corresponding author: liyiyang328@163.com; 1: These authors contributed equally to this work.*

INTRODUCTION

Global energy demand continues to increase, while reserves of non-renewable fossil fuels are gradually being depleted (Bota-Avram *et al*. 2024). Their extensive use has also raised growing environmental concerns. Together, these pressures have accelerated the search for renewable energy alternatives (Moradi *et al*. 2021; Xu and Zhao *et al*. 2023). Bioenergy derived from biomass has attracted particular attention because it offers a renewable and potentially low-carbon source of energy (Kumar *et al*. 2023; El-Fawal *et al*. 2025). Biomass is widely available, biodegradable, renewable, and often relatively inexpensive compared with conventional feedstocks (Ab Rasid *et al*. 2021; Blay-Roger *et al*. 2024). As global agroforestry production increases, a wide variety of forestry waste are left behind. Unlike biomass, which is grown specifically for energy production, forestry waste is a by-product of raw material processing and consumption (Sarker *et al*. 2021). Forestry and wood-processing activities generate large amounts of waste. Some of this

material is discarded or burned, which can pollute the environment. Follow-up research has proved that forestry waste can be used to produce biomass energy, and the use of waste biomass can increase the value of biomass waste, providing it with economic development and sustainability (Woiciechowski *et al*. 2020; Yao *et al*. 2026).

Forestry wastes—including leaves, bark, nut shells, and pruning branches—are generated in large quantities worldwide each year. Much of this material remains poorly utilized. It is often burned in the open, sent to landfills, or combusted inefficiently for energy. Besides wasting a potentially valuable biomass resource, these practices release greenhouse gases and particulate matter, worsening local air pollution and contributing to global climate change (Guo *et al*. 2024; Srivastava *et al*. 2024). Forestry waste is rich in cellulose, hemicellulose, and lignin, making it particularly well suited for bioenergy production (Al-Rajhi *et al*. 2022). Compared with dedicated energy crops, converting forestry waste into energy avoids direct competition with food production for arable land. It may also lower feedstock costs and offers a more environmentally sound approach to managing this waste stream (Nayak *et al*. 2025; Sulis *et al*. 2025). This approach can help conserve resources, reduce pollution, and strengthen energy security (Ungureanu *et al*. 2025). Meanwhile, recent advances in thermochemical technologies including pyrolysis, gasification, and hydrothermal liquefaction along with biochemical processes such as anaerobic digestion and fermentation, have broadened the range of options for utilizing this waste stream efficiently (Li *et al*. 2021). Among the available conversion technologies, pyrolysis is one of the most mature and widely studied. It can produce several value-added products, including bio-oil, biochar, and pyrolysis gas, making it a promising option for biomass utilization (Wang *et al*. 2024). However, forestry waste varies considerably in its physicochemical properties. Its pyrolysis behavior and product distribution are influenced by feedstock composition, operating temperature, heating rate, and the presence of catalysts. A clear understanding of how a specific type of forestry waste responds to pyrolysis is essential for optimizing its conversion and energy recovery (Wang *et al*. 2024).

Plant-derived shells from agricultural and forestry production have attracted increasing attention as feedstocks for sustainable energy and value-added materials (El-Hussieny *et al*. 2020; Al-Rajhi *et al*. 2023; Moawad *et al*. 2026; Alharthi *et al*. 2026). These shells are a form of lignocellulosic biomass and are mainly composed of cellulose, hemicellulose, and lignin (Wang *et al*. 2017; Parakh *et al*. 2020). Lignocellulosic biomass is widely available around the world, and it is an important raw material for bioenergy production (Bhat *et al*. 2024). A variety of plant shells have already been explored for different resource-recovery applications. Coconut shells, for example, can be used as partial replacements for conventional aggregates in structural concrete (Ahmad *et al*. 2022). Their high carbon content also makes them suitable precursors for biochar production (Duc *et al*. 2019). Peanut shells are generated in large quantities as solid by-products of peanut processing and oil production, giving them considerable potential as a low-cost biofuel feedstock (Yurt *et al*. 2022; Al-Rajhi *et al*. 2025). Andiroba shells from the Amazon region have likewise been investigated as an abundant and inexpensive renewable precursor for activated carbon production (Serafin *et al*. 2022). The development of efficient, economically viable, and environmentally benign conversion routes for forestry residues is strategically important for relieving the strain on depleted fossil energy resources, restoring the ecological environment, and facilitating green and low-carbon development.

The authors' group has previously studied leaf pyrolysis and the nanocatalytic pyrolysis of *Aesculus chinensis* (*A. chinensis*) Bunge seeds (Li *et al*. 2021, 2022). Here, the seed shell refers to the outer covering of the seed, whereas the kernel refers to the inner tissue remaining after the shell is removed. The seed shell is a distinct fraction generated

during fruit processing, and studying it may offer a way to use this material while leaving the kernel available for other uses. Its chemical composition should be examined directly rather than inferred from that of the leaves or seeds. To our knowledge, no published study has brought together an analysis of the shell's extractable compounds, functional groups, thermal behavior, and pyrolysis products. Therefore, in this work the extracts were characterized by gas chromatography-mass spectrometry (GC–MS) and Fourier-transform infrared spectroscopy (FT–IR). The shell's thermal behavior was examined by thermogravimetric analysis (TGA), and its pyrolysis products were profiled by pyrolysis-gas chromatography-mass spectrometry (Py/GC–MS). These results provide a preliminary basis for assessing the seed shell's potential as a feedstock for bioenergy or value-added chemical production.

EXPERIMENTAL

Materials

Fresh seeds of *A. chinensis* Bunge were collected in Xixia County, China, and the seed shells were manually separated from the kernels. The shells were frozen to absolute dryness and then crushed to 40 to 60 μm and 200 μm powder. The 40 to 60 μm powder was extracted, and the 200 μm powder was used for TGA and Py/GC–MS analysis.

The 40 to 60 μm powder (15 g) was extracted in 300 mL of organic solvent. The four organic solvents were ethanol, methanol, benzene/ethanol (volume ratio 1:1), and ethanol/methanol (volume ratio 1:1), with extraction temperatures of 75, 65, 90, and 70 °C, respectively. The extraction time was 5 h. The four extractives were concentrated to approximately 20 mL for FT–IR and GC–MS analysis.

Fourier Transform Infrared (FT–IR) Spectroscopy

For FT–IR analysis, approximately 1 mL of each extract was mixed with 1 g of KBr. After the solvent had completely evaporated, the mixture was pressed into a pellet and analyzed using an IR100 Fourier-transform infrared spectrometer (Thermo Nicolet, Madison, WI, USA) (Li *et al*. 2022).

Gas Chromatography–Mass Spectrometry (GC–MS)

The four extractives were analyzed separately using an Agilent 7890B-5977A mass selective detector (Agilent Technologies, Santa Clara, CA, USA). Separation was performed using an HP-5MS fused-silica capillary column (30 m × 0.25 mm × 0.25 μm). High-purity helium was used as the carrier gas at a constant flow rate of 1 mL/min, and the split ratio was 2:1. The initial oven temperature was maintained at 50 °C and then increased to 250 °C at a rate of 8 °C/min, followed by an increase to 300 °C at 5 °C/min. The mass spectrometer was operated in electron ionization mode at an ionization energy of 70 eV and an ionization current of 150 μA. Mass spectra were recorded over an *m*/*z* range of 30 to 600. The ion-source and quadrupole temperatures were maintained at 230 and 150 °C, respectively (Li *et al*. 2023).

Thermogravimetric Analysis (TGA)

Thermogravimetric analysis was conducted using an STA 8000 simultaneous thermal analyzer (PerkinElmer, Waltham, MA, USA). Approximately 1 mg of the 200 μm powder was analyzed under a nitrogen atmosphere at a flow rate of 60 mL/min. The sample was heated from 30 to 300 °C at a rate of 5 °C/min (Li *et al*. 2021).

Pyrolysis-Gas Chromatography–Mass Spectrometry (PY/GC–MS)

The 0.1 mg of 200-mesh powder was analyzed on a pyrolysis Agilent–7890B–5977A CDS5000 (Agilent Technologies, Santa Clara, CA, USA) instrument, with the following parameters: carrier gas, high purity helium; pyrolysis temperature of 500 ℃; heating rate of 20 ℃/ms; pyrolysis time of 15 s; pyrolysis product transfer line and injection valve temperature of 300 ℃; HP–5MS column; capillary column (60 m × 250 μm × 0.25μm); parallel mode, the split ratio 1:60; and shunt speed 50 mL/min. The temperature of the GC program was raised from 40 ℃ for 2 min, raised to 120 ℃ at a rate of 5 ℃ / min, and then raised to 200 ℃ at a rate of 10 ℃/min for 15 min. The ion source (EI) temperature was 230 ℃, and the scanning range was 28 to 500 amu (Li *et al*. 2023).

RESULTS AND DISCUSSION

FT–IR Analysis

The functional groups present in the four *A. chinensis* Bunge seed shell extracts were characterized by FT–IR spectroscopy, and the resulting spectra are compared in Fig. 1. Overall, the four extracts showed broadly similar spectral profiles. Their main absorbance bands were concentrated in the ranges of 3442 to 3363, 2976 to 2898, and 1655 to 881 cm^{-1}, indicating the presence of alcohols and phenols, organic acids and esters, ketones and aldehydes, as well as aliphatic and aromatic compounds (Li *et al*. 2019). The broad band at 3442 to 3363 cm^{-1} was assigned to O–H stretching vibrations, whereas the band near 2976 cm^{-1} was mainly associated with aliphatic C–H stretching. The absorbance band at approximately 1655 cm^{-1} may be attributed to conjugated C=O or aromatic C=C vibrations. Bands at 1456 and 1413 cm^{-1} were related to C–H deformation and aromatic skeletal vibrations. The peaks at 1326, 1272, 1087, and 1049 cm^{-1} were mainly associated with C–O and C–C vibrations, while the band at 881 cm^{-1} may arise from out-of-plane C–H vibrations in substituted aromatic structures (Naim *et al*. 2022). These spectral features suggest that the *A. chinensis* Bunge seed shell extracts contained related lignin-derived and oxygen-containing compounds. Some differences in band intensity were nevertheless observed. In particular, the ethanol and methanol extracts of *A. chinensis* Bunge seed shells showed stronger absorbance near 1655 cm^{-1} but weaker bands at several other positions, including 2976 cm^{-1} (Shannon *et al*. 2022). The methanol extract also exhibited lower transmittance over most of the spectral range, except near 3363 and 1655 cm^{-1} (Soni *et al*. 2022). This indicates relatively stronger overall absorption and may reflect the selective extraction or enrichment of compounds with different functional groups. The observed differences are therefore more reasonably attributed to solvent selectivity than to the hydrolysis of cellulose or lignin.

The FT–IR results showed that the extracts of *A. chinensis* Bunge seed shells contained abundant oxygen-containing functional groups, including hydroxyl, carbonyl, and ether groups, together with aliphatic structures. Differences were observed at 3363, 1655, and 1049 cm^{-1}. These bands were mainly associated with O–H stretching, conjugated C=O or aromatic C=C stretching and the bending vibration of adsorbed water, and C–O stretching, respectively. Their varying intensities indicate that solvents with different polarities selectively extracted compounds containing these functional groups. The ethanol and methanol extracts exhibited weaker absorbance near 2976 cm^{-1}, suggesting a lower relative abundance of aliphatic C–H structures.

Several other characteristic bands also decreased after extraction, suggesting the removal of soluble alcohols, organic acids, esters, and related oxygen-containing compounds. During pyrolysis, relatively labile C–O bonds and aliphatic structures may

contribute to volatile formation, whereas more condensed aromatic structures are more likely to remain in the solid phase and participate in biochar formation. These findings suggest that *A. chinensis* Bunge seed shells have potential for the production of both liquid pyrolysis products and carbon-rich solid materials. Although extraction changed the relative abundance of some functional groups, the remaining material retained aromatic and oxygen-containing structures relevant to thermochemical conversion. The FT–IR analysis supports the potential of *A. chinensis* Bunge seed shells forestry waste as a pyrolysis feedstock for bio-oil and other value-added products, while also providing useful information for the development of an integrated extraction–pyrolysis process.

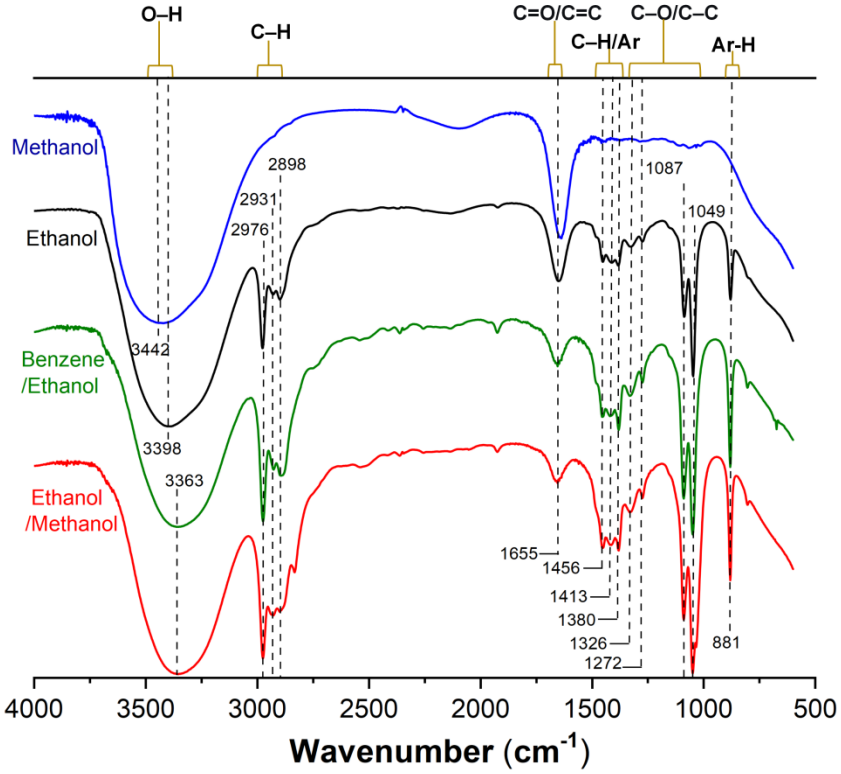


Fig. 1. FT-IR spectra of the four extractives from *A. chinensis* Bunge seed shell. The main absorption bands were assigned to O–H stretching, aliphatic C–H stretching, conjugated C=O or aromatic C=C stretching, C–H deformation and aromatic skeletal vibrations, C–O/C–C vibrations, and out-of-plane C–H vibration of substituted aromatic rings. Ar = aromatic ring.

GC–MS Analysis

The total ion chromatograms of the four extracts analyzed by GC–MS are shown in Supplementary Figure S1. According to the results of GC–MS analysis, *A. chinensis* Bunge seed shell ethanol, methanol, benzene/ethanol, and ethanol/methanol detected 29, 32, 22, and 23 chemical active components, respectively. The contents are shown in Supplementary Tables S1 to S4; they included guanethidine (0.46%), clindamycin (4.13%), acetic acid, hydrazide (0.97%), dl-Arabinose (1.49%), d-Mannose (0.82%), methyl alcohol (0.77%), fenretinide (0.11%), melezitose (2.42%), hydrazinecarboxamide (1.00%), ethyl iso-allocholate (2.54%), 5-Hydroxymethylfurfural (6.18%). The remaining identified compounds showed lower relative peak areas.

Some compounds tentatively identified in the *A. chinensis* Bunge seed-shell extracts have been reported in the literature to possess biological or pharmacological activities. For example, guanethidine is used as an antihypertensive drug, which is a norepinephrine nerve blocker that mainly blocks the release of norepinephrine at nerve

endings. It has a similar effect to ganglion blockers, but without parasympathetic blockade effects (Hertting *et al.* 1962; Owens *et al.* 2021). Guanethidine can also block sympathetic function in primary fibromyalgia skeletal muscle and inhibit the release of acetylcholine (Bäckman *et al.* 1988; Han *et al.* 2026). Clindamycin is clinically used for a variety of infections caused by anaerobic infections or Staphylococcus aureus (Hodille *et al.* 2018). In addition, it has a good effect on the treatment of certain serious infections, such as lung abscess, osteomyelitis, sepsis, and other diseases (Memariani *et al.* 2021).

Acetic acid, hydrazide is an important chemical raw material and pharmaceutical intermediate. It can be used to synthesize analgesic drugs, anti-tuberculosis drugs. (Maridevarmath *et al*. 2019). DL-Arabinose exhibits significant neuroprotective effects during diabetic cerebral ischemia or reperfusion injury, demonstrating that it can act as a useful anti-inflammatory lead compound in the treatment of early diabetic ischemic stroke (Li *et al*. 2021). d-Mannose is a natural bioactive substance with a wide range of applications (Dong *et al*. 2019; Kyriakides *et al*. 2021).

The chemical profiles of the *A. chinensis* Bunge seed shell extracts varied across the different retention-time intervals (Fig. 2). At <10 min, the relative contents of compounds in the four extracts were 5.23, 8.61, 6.19, and 19.52%, respectively. The corresponding values were 11.11, 7.12, 24.17, and 20.72% at 10 to 20 min, and 16.04, 26.35, 9.58, and 17.94% at ≥20 min. Overall, most of the detected compounds were found in the 10 to 20 min and ≥20 min regions, including esters, organic acids, glycoside-related compounds, and other relatively low-volatility constituents. Clear differences were observed among the chemical profiles obtained with the different solvent systems. The methanol extract contained the greatest number of identified compounds, with 38 species, whereas the ethanol/methanol extract showed the highest total relative peak area, reaching 58.18%. Its components were also more evenly distributed across the three retention-time intervals. The ethanol/methanol mixture gave the most balanced profile. The two solvents may have complementary properties and thus extract different sets of compounds.

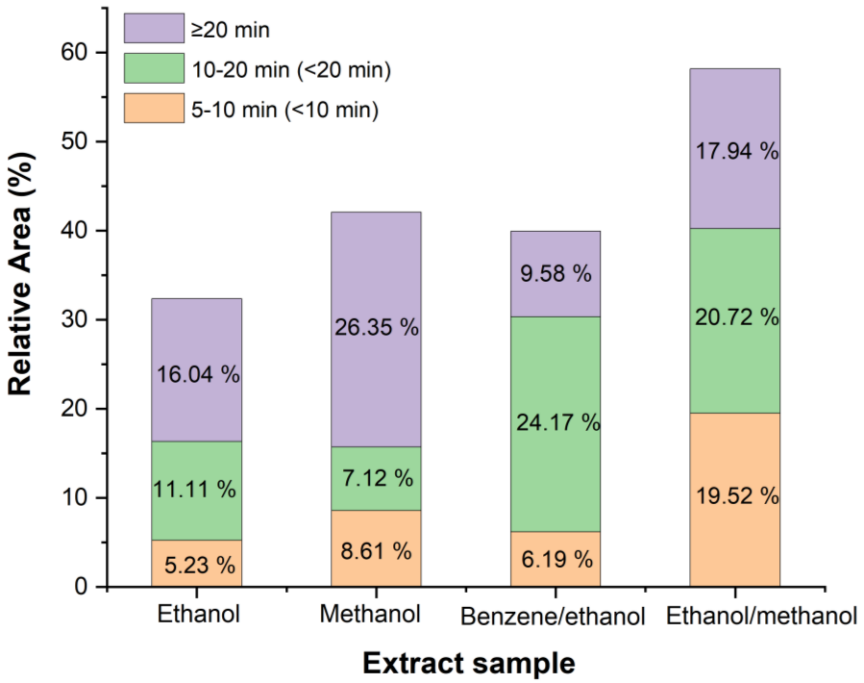


Fig. 2. Distribution characteristics of the four extractives from *A. chinensis* Bunge seed shell by GC–MS. The Y-axis (Relative Area, %) represents the sum of the identified peak areas relative to the total chromatogram area, rather than normalized fractions of 100%.

The results therefore indicate that solvent selection strongly influenced both the number and relative abundance of compounds recovered from *A. chinensis* Bunge seed shells. Among the identified compounds, 5-hydroxymethylfurfural (6.18%) and ethyl iso-allocholate (2.54%) exhibited relatively high abundances. The former serves as an important platform chemical for the synthesis of fuels and fine chemicals, whereas the latter is a steroid derivative with certain pharmaceutical development potential. Furthermore, several compounds previously reported in the literature to have biological activities were tentatively identified, including guanethidine, clindamycin, acetic acid hydrazide, dl-arabinose, and d-mannose. These further substantiate the potential application value of this seed shell extract in the pharmaceutical and chemical industries. Considering the comprehensive evaluation of extraction efficiency, compound diversity, and solvent safety, the ethanol/methanol mixed solvent emerges as a preferable choice for the extraction of active constituents from A. chinensis Bunge seed shell, offering both high extraction yield and low toxicity. This solvent system also provides a clear direction for pretreatment optimization in the subsequent pyrolytic conversion to bio-oil.

TGA Analysis

The thermal degradation behaviour of *A. chinensis* Bunge seed shell was examined by TGA/DTG (Fig. 3) (Song *et al*. 2022). The weight-loss profile showed three distinct stages. The first stage, from 20 to 48 °C, involves a mass loss of about 1 wt.%, which is mainly due to evaporation of surface moisture (Rami *et al*. 2021). The second stage, between 48 and 206 °C, showed a slower and relatively steady mass loss of around 8 wt.%, probably resulting from the initial decomposition of some low-molecular-weight components in the sample (Anca-Couce *et al.* 2020). The third stage, from 206 to 300 °C, was characterised by a more rapid weight loss of 13.9 wt.%, corresponding to the decomposition of cellulose and hemicellulose, which break down extensively as the temperature rises and release large amounts of volatiles (Kanca 2020). The final residual mass was 77.1 wt.%, suggesting that the material loses only a moderate fraction of its mass during pyrolysis.

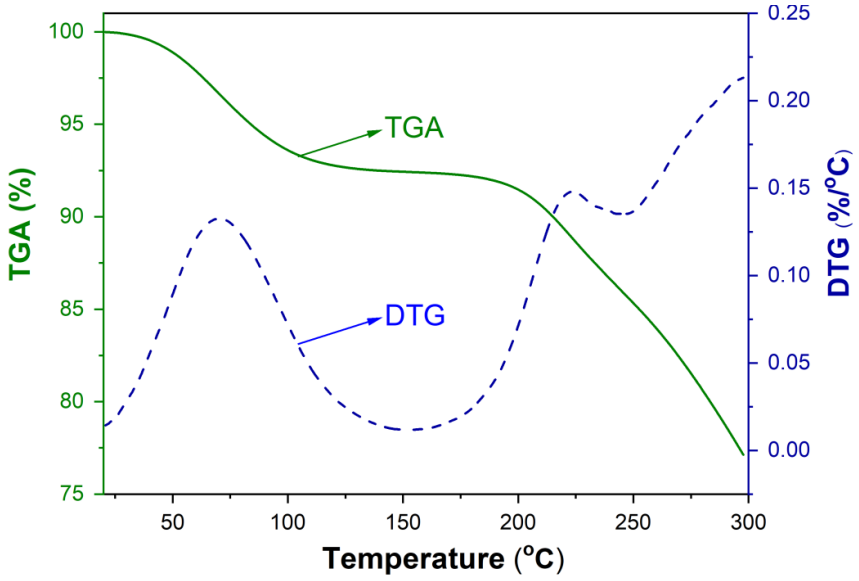


Fig. 3. TGA and DTG thermal curves of *A. chinensis* Bunge seed shell

From a thermal stability perspective, the sample remained fairly stable up to 206 °C, with only minor changes in mass. The major decomposition occurring between 206 and 300 °C indicates that the main organic fractions, primarily cellulose and hemicellulose, were converted within this relatively narrow temperature window. This feature may offer some advantage for selective product recovery through controlled pyrolysis (Wang *et al*. 2019; Voltolini *et al*. 2025). The TGA results showed a gradual mass loss in the seed shell of *A. chinensis* Bunge, with 77.1 wt.% of its initial mass remaining at 300 °C. This indicates that the seed shell has a degree of thermal stability within the temperature range examined in this study and provides a basis for further assessment of its thermal conversion behavior.

PY/GC–MS Analysis

The pyrolysis product components of *A. chinensis* Bunge seed shell were identified by Py/GC–MS technology (Fig. 4). The results show that the pyrolysis products were very rich, and a total of 192 compounds were identified. According to the statistics in Table S5, they were divided into 4 categories: (1) aldehyde ketone (15.33%), (2) acid ester (11.47%), (3) alcohol phenol (32.24%), (4) hydrocarbons (40.96%), of which the proportions of acid (10.31%), ketone (13.66%) and alcohol (27.89%) were high (Fig. 5). Ketone, aldehyde, acid, ester, alcohol, phenol and hydrocarbons were detected 50, 8, 16, 8, 25, 14 and 72 compounds, respectively. Bio-oils are composed of mixtures with high oxygen content, includes almost all organic compounds containing oxygen such as aldehydes ketones, esteric acids, alcohol ethers and so on (Setiabudi *et al*. 2020). The findings indicate that the pyrolysates were predominantly oxygenated compounds, which form the chemical basis for bio-oil precursors.

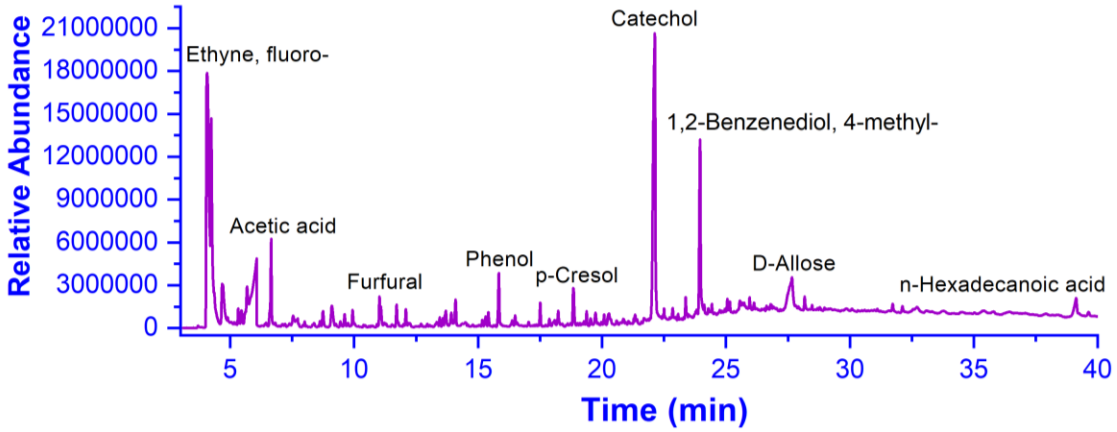


Fig. 4. Total ion chromatogram of pyrolysis products from *A. chinensis* Bunge seed shell by Py/GC–MS

Several identified compounds possess well-established industrial applications. Dodecanoic acid is easy to get and inexpensive, and it can be used in the chemical industry such as alkyd resins, wetting agents, and detergents (Matsuoka *et al*. 2023). Dodecanoic acid has little volume variation, and it can remain stable in hundreds of thermal cycling experiments and become a promising heat storage material (Whitman *et al*. 2013). Octadecanoic acid is widely used in release agents, stabilizers, surfactants, and is a commonly used organic chemical in the chemical industry (Guízar-González *et al*. 2016). n-Hexadecanoic acid is one of the most widely distributed fatty acids in nature; it is mainly used in the plastics industry, lubricants, pharmaceutical industry (Afolayan *et al*. 2024). Furfural, as a key platform chemical derived from lignocellulosic biomass, can be converted *via* green and efficient heterogeneous catalysis into a variety of high-value fuels

and chemicals, thereby playing a significant role in the chemical industry (Yang *et al*. 2024; Zhao *et al*. 2024). This compositional profile suggests that the seed shell not only provides energy-related components (hydrocarbons at 40.96%) but also yields functional oxygenated compounds (alcohols/phenols at 32.24%), offering diversified product streams for biorefinery applications.

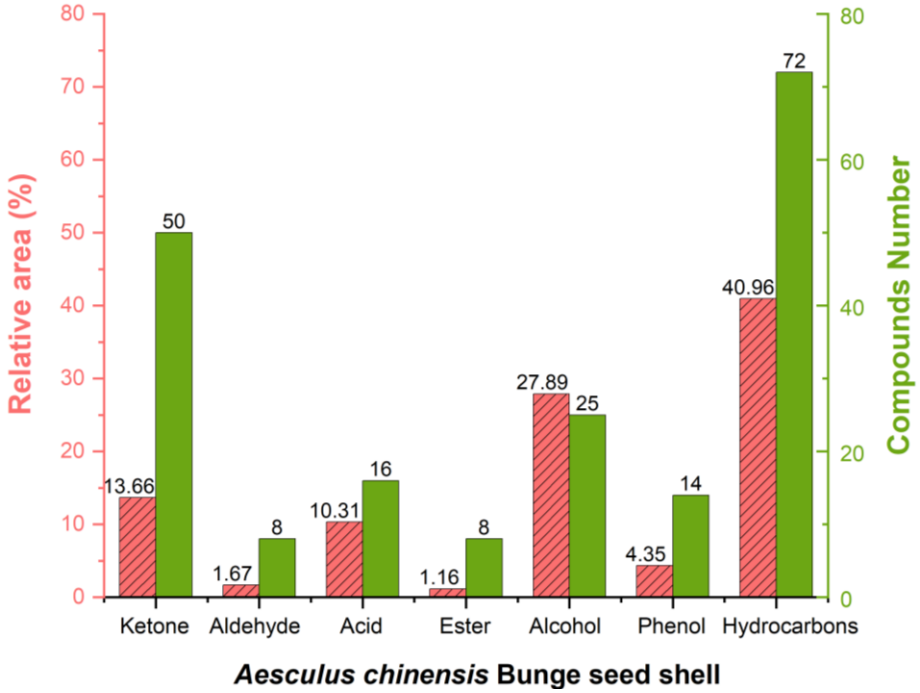


Fig. 5. Distribution characteristics of pyrolysis products from *A. chinensis* Bunge seed shell by Py/GC–MS

From a sustainability perspective, the seed shell considered in this work is a forestry by-product that does not require dedicated cultivation, and its pyrolysis generates a wide range of recoverable compounds. This is consistent with the circular economy model of turning waste into useful products. The presence of commercially established fatty acids and platform chemicals, such as furfural, adds economic value to this feedstock. Taken together, these findings suggest that *A. chinensis* Bunge seed shells could serve both as a bioenergy feedstock and as a potential source of green chemical intermediates. Further investigation is therefore warranted to optimize the conversion process and evaluate its technical and economic feasibility as a forestry-derived biomass resource.

CONCLUSIONS

1. Fourier transform infrared (FT–IR) analysis confirmed the presence of functional groups commonly associated with lignocellulosic biomass, including hydroxyl, carbonyl, ether, aliphatic, and aromatic structures. Gas chromatography-mass spectrometry (GC–MS) tentatively identified 5-hydroxymethylfurfural, ethyl iso-allocholate, guanethidine, and clindamycin in the seed-shell extracts. 5-Hydroxymethylfurfural is a platform chemical for producing fuel intermediates and fine chemicals. Although pharmacological or biological activities have been reported

for some of these compounds, the activity of the extracts themselves was not assessed. The chemical profile supports further valorization of the extracts, while the pharmaceutical relevance of individual constituents remains to be investigated.

2. Thermogravimetric analysis (TGA) was used to characterize the thermal decomposition behavior of the seed shells, while pyrolysis/gas chromatography-mass spectrometry (Py/GC–MS) was used to identify volatile pyrolysis products, including ketones, organic acids, alcohols, and other oxygen-containing compounds. These findings provide preliminary information on the shell's thermochemical conversion behavior, but further product-yield and energy assessments are needed to determine its practical energy potential.
3. Overall, the chemical and pyrolysis profiles suggest that *A. chinensis* Bunge seed shells could be explored as a source of chemical intermediates and as a candidate for thermochemical conversion. Their valorization offers a possible route to higher-value use of this forestry waste.
4. This assessment is preliminary. The yields and properties of the bio-oil, biochar, and pyrolysis gas remain to be determined. Future work should quantify the products, assess their quality, and optimize pyrolysis temperature, heating rate, residence time, and other operating conditions. Techno-economic and environmental assessments will also be needed to determine whether large-scale application is feasible.

ACKNOWLEDGMENTS

The authors are grateful for the support by the Henan Provincial Soft Science Research Project (No. 262400410132) and the College-level Project of Henan Vocational College of Agricultural (No. 2505RCLX07).

Conflict of Interest

The authors declare that they have no known competing financial interests or personal relationships that could have appeared to influence the work reported in this paper.

REFERENCES CITED

Ab Rasid, N. S., Shamjuddin, A., Rahman, A.Z., and Amin, N. A. (2021). "Recent advances in green pre-treatment methods of lignocellulosic biomass for enhanced biofuel production," *J. Cleaner Prod*. 321, article 129038. https://doi.org/10.1016/j.jclepro.2021.129038

Afolayan, F. I. D., Odeyemi, R. A., and Salaam, R. A. (2024). "*In silico* and *in vivo* evaluations of multistage antiplasmodial potency and toxicity profiling of n-hexadecanoic acid derived from *Vernonia amygdalina*," *Front. Pharmacol*. 15, article 1445905. https://doi.org/10.3389/fphar.2024.1445905

Ahmad, R. K., Sulaiman, S. A., Yusup, S., Dol, S. S., Inayat, M., and Umar, H. A. (2022). "Exploring the potential of coconut shell biomass for charcoal production," *Ain Shams Eng. J*. 13(1), article 101499. https://doi.org/10.1016/j.asej.2021.05.013

Al-Rajhi, A., Alharbi, A. A., Yahya, R., and Abdel Ghany, T. M. (2022). "Induction of hydrolytic enzyme production and antibiosis via a culture of dual fungal species

isolated from soil rich with the residues of woody plants in Saudi Arabia," *BioResources* 17(2), 2358-2371. https://doi.org/10.15376/biores.17.2.2358-2371

Al-Rajhi, A. M. H., and Abdelghany, T. M. (2023). "Fiber wastes of date palm for bioethanol production in Saudi Arabia," *BioResources* 18(4), 6827-6841. https://doi.org/10.15376/biores.18.4.6827-6841

Al-Rajhi, A. M. H., Abdelghany, T. M., Selim, S., Almuhayawi, M. S., Alruhaili, M. H., Alharbi, M. T., and Al Jaouni, S. K. (2025). "Phytochemical characterization of peanut oil and its ozonized form to explore biological activities in vitro," *AMB Express* 15, article 76. https://doi.org/10.1186/s13568-025-01849-x

Alharthi, F., Althagafi, H. A., Jafri, I., Alqahtani, L. S., Althagafi, H., Oyouni, A. A. A., Alghamdi, A. A. A., Almotayri, A. M., AlOmari, F., and Naguib, D. M. (2026). "Molecular mechanism of anticancer activity of selected coastal marsh plants from Saudi Arabia," *3 Biotech* 16(4), article 120. https://doi.org/10.1007/s13205-025-04686-8 PubMed

Anca-Couce, A., Tsekos, C., Retschitzegger, S., Zimbardi, F., Funke, A., Banks, S., Kraia, T., Marques, P., Scharler, R., de Jong, W., and Kienzl, N. (2020). "Biomass pyrolysis TGA assessment with an international round robin," *Fuel* 276, article 118002. https://doi.org/10.1016/j.fuel.2020.118002

Bäckman, E., Bengtsson, A., Bengtsson, M., Lennmarken, C., and Henriksson, K.-G. (1988). "Skeletal muscle function in primary fibromyalgia. Effect of regional sympathetic blockade with guanethidine," *Acta Neurol. Scand*. 77(3), 187-191. https://doi.org/10.1111/j.1600-0404.1988.tb05893.x

Bhat, M. A., Bhat, M. A., Jan, S., Shah, A. A., and Jan, A. T. (2024). "Lignocellulosic biomass in circular economy: A techno-transition in carbon neutrality towards sustainable energy production," *Biomass and Bioenergy* 189, article 107349. https://doi.org/10.1016/j.biombioe.2024.107349

Blay-Roger, R., Saif, M., Bobadilla, L. F., Reina, T. R., Nawaz, M. A., and Odriozola, J. A. (2024). "Embracing the sustainable horizons through bioenergy innovations: a path to a sustainable energy future," *Front. Chem*. 12, article 1416102. https://doi.org/10.3389/fchem.2024.1416102

Boţa-Avram, C., Apostu, S. A., Ivan, R., and Achim, M. V. (2024). Exploring the impact of macro-determinant factors on energy resource depletion: Evidence from a worldwide cross-country panel data analysis," *Energy Economics* 130, article 107341. https://doi.org/10.1016/j.eneco.2024.107341

Dong, Z., Wang, Q., Huo, M., Zhang, N., Li, B., Li, H., Xu, Y., Chen, M., Hong, H., and Wang, Y. (2019). "Mannose-modified multi-walled carbon nanotubes as a delivery nanovector optimizing the antigen presentation of dendritic cells," *Chemistryopen* 8(7), 915-921. https://doi.org/10.1002/open.201900126

Duc, P. A., Dharanipriya, P., Velmurugan, B. K., and Shanmugavadivu, M. (2019). "Groundnut shell – A beneficial bio-waste," *Biocatal. Agric. Biotechnol*. 20, article 101206. https://doi.org/10.1016/j.bcab.2019.101206

El-Fawal, E. M., El Naggar, A. M. A., El-Zahhar, A. A., Alghandi, M. M., Morshedy, A.S., El Sayed, H. A., and Mohammed, A. E. M. E. (2025). "Biofuel production from waste residuals: Comprehensive insights into biomass conversion technologies and engineered biochar applications," *RSC Adv*. 15(15), 11942-11974. https://doi.org/10.1039/d5ra00857c

El-Hussieny, N., Bakri, M., Ganash, M., and Abdel Ghany, T. (2020). "Chemical mutagenesis of *Saccharomyces cerevisiae* for enhancing bioethanol production with

fermentation at very high sugar concentration," *BioRes*ources 15(1), 1354-1369. https://doi.org/10.15376/biores.15.1.1354-1369

Guízar-González, C., Monforte-González, M., and Vázquez-Flota, F. (2016). "Yeast extract induction of sanguinarine biosynthesis is partially dependent on the octadecanoic acid pathway in cell cultures of *Argemone mexicana* L. the Mexican poppy," *Biotechnol. Lett*. 38(7), 1237-1242. https://doi.org/10.1007/s10529-016-2095-2

Guo, J. H., Zhang, Y., Fang, J. J., Ma, Z. W., Li, C., Yan, M. Y., Qiao, N. X., Liu, Y., and Bian, M. M. (2024). "Reduction and reuse of forestry and agricultural bio-waste through innovative green utilization approaches: A review," *Forests* 15(8), article 1372. https://doi.org/10.3390/f15081372

Han, X., Jiang, X., Liu, Y., and Chen, G. (2026). "The impact of guanethidine-induced sympathectomy on satellite glial cell activation in a rat model of neuropathic pain," *Neurosci. Lett*. 872, article 138483. https://doi.org/10.1016/j.neulet.2025.138483.

Hertting, G., Axelrod, J., and Patrick, R. W. (1962). "Actions of bretylium and guanethidine on the uptake and release of [^{3}H]-noradrenaline," *Brit. J. Pharmacol*. 18(1), 161-166. https://doi.org/10.1111/j.1476-5381.1962.tb01159.x

Hodille, E., Badiou, C., Bouveyron, C., Bes, M., Tristan, A., Vandenesch, F., Lina, G., and Dumitrescu, O. (2018). "Clindamycin suppresses virulence expression in inducible clindamycin-resistant *Staphylococcus aureus* strains," *Ann. Clin. Microbiol. Antimicrob*. 17, 38. https://doi.org/10.1186/s12941-018-0291-8

Kanca, A. (2020). "Investigation on pyrolysis and combustion characteristics of low quality lignite, cotton waste, and their blends by TGA-FTIR," *Fuel* 263, article 116517. https://doi.org/10.1016/j.fuel.2019.116517

Kumar, S., Darshna, A., and Ranjan, D. (2023). "A review of literature on the integration of green energy and circular economy," *Heliyon* 9(11), article e21091. https://doi.org/10.1016/j.heliyon.2023.e21091

Kyriakides, R., Jones, P., and Somani, B. K. (2021). "Role of D-mannose in the prevention of recurrent urinary tract infections: Evidence from a systematic review of the literature," *Eur. Urol. Focus* 7(5), 1166-1169. https://doi.org/10.1016/j.euf.2020.09.004

Li, Y., Ma, Q., Li, G., Lou, J., Chen, X., He, Y., and Peng, W. (2022). "Pyrolysis of *Aesculus chinensis* Bunge leaves as for extracted bio-oil material," *Polymers* 14(22), article 5003. https://doi.org/10.3390/polym14225003

Li, Y., Liu, E., Gu, H., Lou, J., Yang, Y., Ban, L., Peng, W., and Ge, S. (2023). "Potential of Staphylea holocarpa wood for renewable bioenergy," *Molecules* 28(1), article 299. https://doi.org/10.3390/molecules28010299

Li, H., Ding, R., Shan, Y., Ye, F., Lin, Y., Men, X., Chen, C., Tan, S., Wang, Q., and Hu, B. (2021). "L-arabinose alleviates diabetes-aggravated cerebral ischemic injury by repairing the blood-brain barrier *via* downregulating NF-κB signals," *J. Funct. Foods* 87, article 104839. https://doi.org/10.1016/j.jff.2021.104839

Li, W., Xie, X. A., Sun, J., Fan, D., and Wei, X. (2019). "Investigation of cornstalk cellulose liquefaction in supercritical acetone by FT-TR and GC-MS methods," *Green Chem. Lett. Rev*. 12(3), 299-309. https://doi.org/10.1080/17518253.2019.1643928

Li, Y. Y., Shaheen, S. M., Rinklebe, J., Ma, N. L., Yang, Y. F., Ashraf, M. A., Chen, X. M., and Peng, W. X. (2021). "Pyrolysis of *Aesculus chinensis* Bunge seed with Fe_2O_3/NiO as nanocatalysts for the production of bio-oil material," *J. Hazard.*

Mater. 416, article 126012. https://doi.org/10.1016/j.jhazmat.2021.126012

Maridevarmath, C.V., Naik, L., Negalurmath, V. S., Basanagouda, M., and Malimath, G.H. (2019). "Synthesis, characterization and photophysical studies on novel benzofuran-3-acetic acid hydrazide derivatives by solvatochromic and computational methods," *J. Mol. Struct*. 1188, 142-152. https://doi.org/10.1016/j.molstruc.2019.03.063

Matsuoka, K., and Asamoto, D. (2023). "Preferential removal of alkali metal using dodecanoic acid and sodium dodecyl sulfate in foam separation system," *J. Oleo Sci*. 72(5), 543-548. https://doi.org/10.5650/jos.ess22422

Memariani, M., Memariani, H., and Moravvej, H. (2021). "Inducible clindamycin resistance among clinical *Staphylococcus aureus* strains in Iran: A contemporaneous systematic review and meta-analysis," *Gene Rep*. 23, article 101104. https://doi.org/10.1016/j.genrep.2021.101104

Moradi, P., Saidi, M., and Najafabadi, A. T. (2021). "Biodiesel production via esterification of oleic acid as a representative of free fatty acid using electrolysis technique as a novel approach: Non-catalytic and catalytic conversion," *Process Saf. Environ. Protect*. 147, 684-692. https://doi.org/10.1016/j.psep.2020.12.032

Moawad, H., Alsalamah, S. A., Alghonaim, M. I., Abudayah, W., El-Naggar, M. A., and Almotayri, A. M. (2026). "Enzyme-assisted valorization of plant bioresources for functional bioproducts: A review," *BioResources* 21(2), 5450-5467. https://doi.org/10.15376/biores.21.2.Moawad

Naim, N., Ennahli, N., Hanine, H., Lahlali, R., Tahiri, A., Fauconnier, M., Madani, I., and Ennahli, S. (2022). "ATR-FTIR spectroscopy combined with DNA barcoding and GC-MS to assess the quality and purity of saffron (*Crocus sativus* L.)," *Vib. Spectrosc*. 123, article 103446. https://doi.org/10.1016/j.vibspec.2022.103446

Nayak, A., Bhatt, R., and Bhushan, B. (2025). "Technological challenges, research advancements and future prospects towards valorization of pine wastes," *Biomass Bioenergy* 204, article 108413. https://doi.org/10.1016/j.biombioe.2025.108413

Owens, C., Gasper, W. J., Seward, K., Misra, S., Jacobson, S. B., and Jones, R. M. (2021). "PS222. Percutaneous peri-adventitial guanethidine delivery induces renal artery sympathectomy: Preclinical experience and implication for refractory hypertension," *J. Vasc. Surg*. 53, 87S. https://doi.org/10.1016/J.JVS.2011.03.168

Parakh, P. D., Nanda, S., and Kozinski, J. A. (2020). "Eco-friendly transformation of waste biomass to biofuels," *Curr. Biochem. Eng*. 6(2), 120-134. https://doi.org/10.2174/2212711906999200425235946

Rami, J. M., Patel, C. D., Patel, C. M., and Patel, M. V. (2021). "Thermogravimetric analysis (TGA) of some synthesized metal oxide nanoparticles," *Mater. Today* 43, 655-659. https://doi.org/10.1016/j.matpr.2020.12.554

Sarker, T. R., Pattnaik, F., Nanda, S., Dalai, A. K., Meda, V., and Naik, S. (2021). "Hydrothermal pretreatment technologies for lignocellulosic biomass: a review of steam explosion and subcritical water hydrolysis," *Chemosphere* 284, article 131372. https://doi.org/10.1016/j.chemosphere.2021.131372

Serafin, J. L., Ouzzine, M., Xing, C. C., El Ouahabi, H., Kaminska, A., and Srenscek-Nazzal, J. (2022). "Activated carbons from the Amazonian biomass andiroba shells applied as a CO_2 adsorbent and a cheap semiconductor material," *J. CO2 Util*. 62, article 102071. https://doi.org/10.1016/j.jcou.2022.102071

Setiabudi, H. D., Aziz, M. A. A., Abdullah, S., Teh, L.P., and Jusoh, R. (2020). "Hydrogen production from catalytic steam reforming of biomass pyrolysis oil or

bio-oil derivatives: A review," *Int. J. Hydrogen Energy* 45(36), 18376-18397. https://doi.org/10.1016/j.ijhydene.2019.10.141

Shannon, M., Lafeuille, J. L., Fregiere-Salmomon, A., Lefevre, S., Galvin-King, P., Haughey, S. A., Burns, D. T., Shen, X. Q., Kapil, A., McGrath, T. F., and Elliott, C.T. (2022). "The detection and determination of adulterants in turmeric using fourier-transform infrared (FTIR) spectroscopy coupled to chemometric analysis and micro-FTIR imaging," *Food Control* 139, article 109093. https://doi.org/10.1016/j.foodcont.2022.109093

Song, G. X., Huang, D. X., Li, H. J., Wang, X. P., Ren, Q. Q., Jiang, L., Wang, Y., Su, S., Hu, S., and Xiang, J. (2022). "Pyrolysis reaction mechanism of typical Chinese agriculture and forest waste pellets at high heating rates based on the photo-thermal TGA," *Energy* 244(1), article 123164. https://doi.org/10.1016/j.energy.2022.123164

Soni, A., Yusuf, M., Mishra, V. K., and Beg, M. (2022). "An assessment of thermal impact on chemical characteristics of edible oils by using FTIR spectroscopy," *Mater. Today* 68, 710-716. https://doi.org/10.1016/j.matpr.2022.05.568

Srivastava, N., Singh, P., Srivastava, M., Lal, B., Singh, R., Ahmad, I., and Gupta, V. K. (2024). "A review on the scope and challenges of *Saccharum spontaneum* waste in the context of lignocellulosic biomass for sustainable bioenergy applications," *Renew. Sustain. Energy Rev*. 199, article 114477. https://doi.org/10.1016/j.rser.2024.114477

Sulis, D. B., Lavoine, N., Sederoff, H., Jiang, X., Marques, B. M., Lan, K., Cofre-Vega, C., Barrangou, R., and Wang, J.P. (2025). "Advances in lignocellulosic feedstocks for bioenergy and bioproducts," *Nat. Commun*. 16(1), article 1244. https://doi.org/10.1038/s41467-025-56472-y

Ungureanu, N., Vlăduț, N. V., Biriș, S. Ș., Gheorghiță, N. E., and Ionescu, M. (2025). "Biomass pyrolysis pathways for renewable energy and sustainable resource recovery: A critical review of processes, parameters, and product valorization," *Sustainability* 17(17), article 7806. https://doi.org/10.3390/su17177806

Voltolini, L., Lima, F. A. R. D., Rebello, C. M., Itabaiana, I., Nogueira, I. B. R., Secchi, A. R., and de Souza, M. B. (2025). "Machine learning framework to predict product distribution of lignocellulosic biomass pyrolysis," *Bioresource Technology* 434, article 132746. https://doi.org/10.1016/j.biortech.2025.132746

Wang, B., Xu, F., Zong, P., Zhang, J., Tian, Y., and Qiao, Y. (2019). "Effects of heating rate on fast pyrolysis behavior and product distribution of Jerusalem artichoke stalk by using TG-FTIR and Py-GC/MS," *Renew. Energ*. 132, 486-496. https://doi.org/10.1016/j.renene.2018.08.021

Wang, S., Dai, G., Yang, H., and Luo, Z. (2017). "Lignocellulosic biomass pyrolysis mechanism: a state-of-the-art review," *Prog. Energy Combust. Sci*. 62, 33-86. https://doi.org/10.1016/j.pecs.2017.05.004

Wang, Y., Yang, S.L., Bao, G.R., and Wang, H. (2024). "Pyrolytic characteristics of abutilon stalk waste using TG-FTIR, Py-GC/MS, and artificial neural networks: Kinetics, thermodynamics, and gaseous products distribution," *J. Anal. Appl. Pyrolysis* 178, article 106403. https://doi.org/10.1016/j.jaap.2024.106403

Wang, Z. W., Guo, S. H., Chen, G. F., Zhang, M. J., Sun, T. L., Wang, Q., Zhu, H. N., Yang, S. H., Chen, Y., Wu, M. G., Lei, T. Z., Burra, K. G., and Gupta, A. K. (2024). "Co-pyrolysis of waste tire with agricultural and forestry residues: Pyrolysis behavior, products distribution and synergistic effects," *J. Energy Inst*. 114, article 101634. https://doi.org/10.1016/j.joei.2024.101634

Whitman, C.A., Groulx, D., and White, M. A. (2013). "Dodecanoic acid as a promising phase-change material for thermal energy storage," *Appl. Therm. Eng*. 53(1), 37-41. https://doi.org/10.1016/j.applthermaleng.2012.12.031

Woiciechowski, A. L., Neto, C. J., de Souza, V. L. P., de Carvalho, N. D. P., Sydney, A. C., Letti, L. A., Karp, S. G., Torres, L. A., and Soccol, C. R. (2020). "Lignocellulosic biomass: Acid and alkaline pretreatments and their effects on biomass recalcitrance-conventional processing and recent advances," *Bioesource Technol*. 304, article 122848. https://doi.org/10.1016/j.biortech.2020.122848

Xu, Y., and Zhao, F. (2023). "Impact of energy depletion, human development, and income distribution on natural resource sustainability," *Resour. Policy* 83, article 103531. https://doi.org/10.1016/j.resourpol.2023.103531

Yang, R., Zhang, H. T., Li, X. D., Ye, X. G., and Liu, L. (2024). "When furfural meets Piancatelli rearrangement," *ACS Sustainable Chem. Eng*. 12(33), 12378-12385. https://doi.org/10.1021/acssuschemeng.4c02672

Yao, X., Yuan, W. Y., Wu, S. H., Wang, X., Niu, X. Y., Li, Q. H., Feng, X. D., and Ma, Y.F. (2026). "Remediation of petroleum-contaminated soil using a combination of single and mixed agricultural and forestry wastes with exogenous microorganisms," *Environ. Toxicol. Chem*. 45(7), 2024-2036. https://doi.org/10.1093/etojnl/vgag051

Yurt, U., and Bekar, F. (2022). "Comparative study of hazelnut-shell biomass ash and metakaolin to improve the performance of alkali-activated concrete: A sustainable greener alternative," *Constr. Build. Mater*. 320, article 126230. https://doi.org/10.1016/j.conbuildmat.2021.126230

Zhao, K. Y., Wen, B., Tang, Q., Wang, F., Liu, X. X., Xu, Q., and Yin, D. L. (2024). "Recent catalytic innovations in furfural transformation," *Green Chem*. 26, 9957-9992. https://doi.org/10.1039/d4gc01983k

Article submitted: August 11, 2026; Peer review completed: October 24, 2026; Article accepted: November 6, 2026; Published: November 17, 2026.
DOI: 10.15376/biores.22.1.380-405

APPENDIX

Supplementary Figure S1 and GC–MS Data

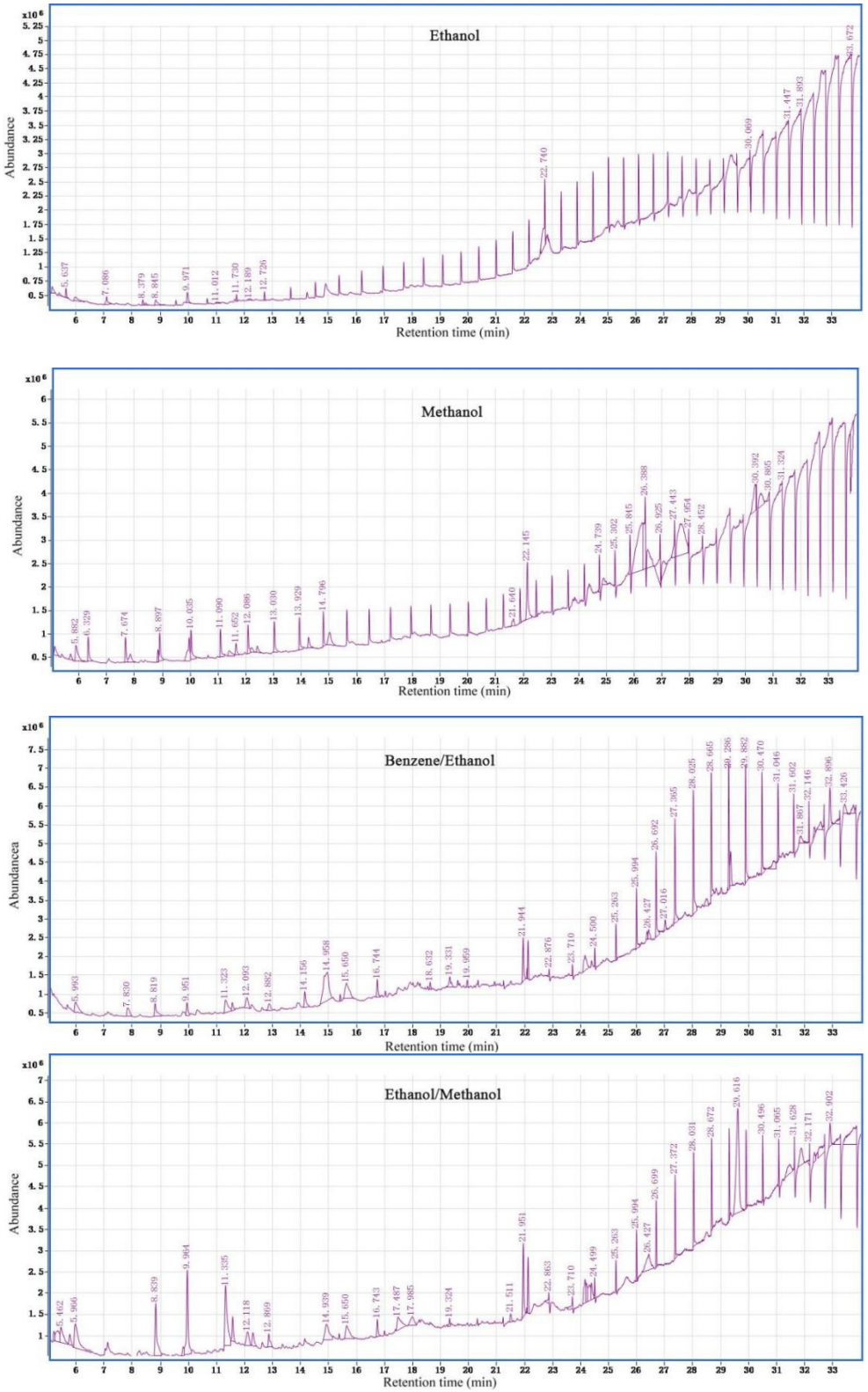


Fig. S1. Total ion chromatogram of the four extractives from *A. chinensis* Bunge seed shell by GC–MS

Table S1. GC-MS Analysis of Ethanol Sample

No.	Retention Time (min)	Peak Area (%)	Component
1	5.14	0.61	DL-Arabinose
2	5.39	0.25	[1,1'-Bicyclopropyl]-2-octanoic acid, 2'-hexyl-, methyl ester
3	5.64	0.49	Acetic acid, hydroxy-, ethyl ester
4	5.95	0.84	DL-Arabinose
5	7.09	0.81	DL-Arabinose
6	8.38	0.28	DL-Arabinose
7	8.48	0.28	Imidazole, 2-amino-5-[(2-carboxy)vinyl]-
8	8.85	0.85	Imidazole, 2-amino-5-[(2-carboxy)vinyl]-
9	9.97	0.82	d-Mannose
10	11.01	0.22	R-Limonene
11	11.73	0.28	R-Limonene
12	12.19	0.28	Tetraacetyl-d-xylonic nitrile
13	14.25	0.43	7-Methyl-Z-tetradecen-1-ol acetate
14	14.91	2.97	[1,1'-Bicyclopropyl]-2-octanoic acid, 2'-hexyl-, methyl ester
15	15.79	0.42	5,6,7,8,9,10-Hexahydro-9-methyl-spiro[2H-1,3-benzoxazine-4,1'-cyclohexane]-2-thione
16	16.96	1.18	Hydrazinecarboxamide
17	17.70	1.11	Hydrazinecarboxamide
18	17.97	0.55	Acetamide, N-methyl-N-[4-(3-hydroxypyrrolidinyl)-2-butynyl]-
19	18.41	1.05	Hydrazinecarboxamide
20	19.09	1.35	Hydrazinecarboxamide
21	19.75	1.27	Hydrazinecarboxamide
22	20.39	1.32	Hydrazinecarboxamide
23	21.00	1.59	Hydrazinecarboxamide
24	21.60	1.71	Hydrazinecarboxamide
25	22.18	1.61	Acetic acid, hydroxy-
26	22.74	5.01	5H-Benzo[b]pyran-8-ol, 2,3,5,5,8a-pentamethyl-6,7,8,8a-tetrahydro-
27	22.83	0.27	2-[4-methyl-6-(2,6,6-trimethylcyclohex-1-enyl)hexa-1,3,5-trienyl]cyclohex-1-en-1-carboxaldehyde
28	23.32	2.18	Acetic acid, hydroxy-
29	23.89	2.35	Acetic acid, hydroxy-

Table S2. GC-MS Analysis of Methanol Sample

No.	Retention Time (min)	Peak Area (%)	Component
1	5.12	0.59	DL-Arabinose
2	5.69	0.36	DL-Arabinose
3	5.88	1.49	DL-Arabinose
4	6.33	1.00	Hydrazinecarboxamide
5	7.67	0.97	Acetic acid, hydrazide
6	7.84	0.80	3-Trifluoroacetoxydodecane
7	8.84	0.46	Guanethidine
8	8.90	1.23	2-Amino-4-hydroxylaminopyrimidine
9	9.96	1.71	Melibiose
10	10.04	1.39	DL-Arabinose
11	11.42	0.58	R-Limonene
12	11.65	0.53	R-Limonene
13	12.21	0.37	R-Limonene
14	12.42	0.42	R-Limonene
15	14.27	0.57	Furan-2-carbohydrazide, N2-(3-indolylmethylene)-
16	15.02	1.33	1,2-Cyclopentanedicarboxylic acid, 4-(1,1-dimethylethyl)-, dimethyl ester, (1.alpha.,2.beta.,4.beta.)-
18	18.08	0.47	Acetamide, N-methyl-N-[4-(3-hydroxypyrrolidinyl)-2-butynyl]-
19	21.64	0.46	2-[4-methyl-6-(2,6,6-trimethylcyclohex-1-enyl)hexa-1,3,5-trienyl]cyclohex-1-en-1-carboxaldehyde
20	22.15	2.89	Estra-1,3,5(10)-trien-17.beta.-ol
21	23.03	0.73	Hydrazinecarboxamide
22	23.61	0.76	Hydrazinecarboxamide
23	23.79	0.26	2-[4-methyl-6-(2,6,6-trimethylcyclohex-1-enyl)hexa-1,3,5-trienyl]cyclohex-1-en-1-carboxaldehyde
24	23.85	0.41	2-[4-methyl-6-(2,6,6-trimethylcyclohex-1-enyl)hexa-1,3,5-trienyl]cyclohex-1-en-1-carboxaldehyde
25	24.20	0.77	Methyl Alcohol
26	25.30	0.60	Methyl Alcohol
27	25.85	0.86	Cedran-diol, (8S,14)-
28	26.39	3.75	2-[4-methyl-6-(2,6,6-trimethylcyclohex-1-enyl)hexa-1,3,5-trienyl]cyclohex-1-en-1-carboxaldehyde
29	26.93	2.76	2-[4-methyl-6-(2,6,6-trimethylcyclohex-1-enyl)hexa-1,3,5-trienyl]cyclohex-1-en-1-carboxaldehyde
30	27.65	7.86	Butanoic acid, 1a,2,5,5a,6,9,10,10a-octahydro-5,5a-dihydroxy-4-(hydroxymethyl)-1,1,7,9-tetramethyl-11-oxo-1H-2,8a-methanocyclopenta[a]cyclopropa[e]cyclodecen-6-yl ester, [1aR-(1a.alpha.,2.alpha.,5.beta.,5a.beta.,6.beta.,8a.alpha.,9.alpha.,10a.alpha.)]-

No.	Retention Time (min)	Peak Area (%)	Component
31	27.95	0.27	2-[4-methyl-6-(2,6,6-trimethylcyclohex-1-enyl)hexa-1,3,5-trienyl]cyclohex-1-en-1-carboxaldehyde
32	28.45	0.11	Fenretinide

Table S3. GC-MS Analysis of Benzene/ethanol Sample

No.	Retention Time (min)	Peak Area (%)	Component
1	5.99	2.11	6-Methyl-3-phenethylsulfanyl-[1,2,4]triazin-5-ol
2	7.83	1.19	3-Trifluoroacetoxypentadecane
3	8.82	1.69	Acetic acid, 6-morpholin-4-yl-9-oxobicyclo[3.3.1]non-3-yl ester
4	9.95	1.20	.beta.-D-Glucopyranose, 4-O-.beta.-D-galactopyranosyl-
5	11.32	2.42	Melezitose
6	11.57	0.77	Melezitose
7	12.09	1.61	Melezitose
8	12.88	1.02	Melezitose
9	14.16	1.58	Furan-2-carbohydrazide, N2-(3-indolylmethylene)-
10	14.96	9.21	Melezitose
11	15.42	0.28	[1,1'-Bicyclopropyl]-2-octanoic acid, 2'-hexyl-, methyl ester
12	15.65	3.98	Melezitose
13	16.74	1.23	(3,3-Dimethyl-5-methylthio-3,4(2H)-dihydropyrrol-2-ylidene)acetonitrile
14	18.63	0.39	Perhydrocyclopropa[e]azulene-4,5,6-triol, 1,1,4,6-tetramethyl
15	19.33	1.30	1b,4a-Epoxy-2H-cyclopenta[3,4]cyclopropa[8,9]cycloundec[1,2-b]oxiren-5(1aH)-one, 2,7,9,10-tetrakis(acetyloxy)decahydro-3,6,8,8,10a-pentamethyl-
16	19.96	0.38	1b,4a-Epoxy-2H-cyclopenta[3,4]cyclopropa[8,9]cycloundec[1,2-b]oxiren-5(1aH)-one, 2,7,9,10-tetrakis(acetyloxy)decahydro-3,6,8,8,10a-pentamethyl-
17	21.94	2.54	Ethyl iso-allocholate
18	22.13	1.76	1,2-Benzenedicarboxylic acid, butyl octyl ester
19	24.50	0.54	Pyrazole[4,5-b]imidazole, 1-formyl-3-ethyl-6-.beta.-d-ribofuranosyl-
20	25.26	1.30	Benzeneethanamine, 2,5-difluoro-.beta.,3,4-trihydroxy-N-methyl-
21	29.35	2.55	Pyrazole[4,5-b]imidazole, 1-formyl-3-ethyl-6-.beta.-d-ribofuranosyl-
22	32.15	0.89	1,4-Bis(trimethylsilyl)benzene

Table S4. GC-MS Analysis of Ethanol/methanol Sample

No.	Retention Time (min)	Peak Area (%)	Component
1	5.20	0.49	DL-Arabinose
2	5.33	1.65	DL-Arabinose
3	5.46	1.94	Levoglucosenone
4	5.77	0.71	o-Acetyl-L-serine
5	5.97	4.23	DL-Arabinose
6	8.84	4.13	Clindamycin
7	9.82	0.52	Melezitose
8	9.96	5.85	4H-Pyran-4-one, 2,3-dihydro-3,5-dihydroxy-6-methyl-
9	11.34	6.18	5-Hydroxymethylfurfural
10	11.58	1.31	Melezitose
11	12.12	1.60	Melezitose
12	12.31	1.08	Melezitose
13	12.87	0.98	Melezitose
14	14.94	2.67	Melezitose
15	15.65	2.10	Melezitose
16	16.74	0.84	Acetamide, N-methyl-N-[4-(3-hydroxypyrrolidinyl)-2-butynyl]-
17	17.49	2.22	Acetamide, N-methyl-N-[4-(3-hydroxypyrrolidinyl)-2-butynyl]-
18	17.99	1.38	Acetamide, N-methyl-N-[4-(3-hydroxypyrrolidinyl)-2-butynyl]-
19	19.32	0.36	1b,4a-Epoxy-2H-cyclopenta[3,4]cyclopropa[8,9]cycloundec[1,2-b]oxiren-5(1aH)-one, 2,7,9,10-tetrakis(acetyloxy)decahydro-3,6,8,8,10a-pentamethyl-
20	21.95	3.11	Estra-1,3,5(10)-trien-17.beta.-ol
21	22.13	1.91	1,2-Benzenedicarboxylic acid, butyl octyl ester
22	25.26	0.62	Pyrazole[4,5-b]imidazole, 1-formyl-3-ethyl-6-.beta.-d-ribofuranosyl-
23	29.62	12.30	Vitamin E

Supplementary Py–GC–MS Data

Table S5. Pyrolysis Products of *A. chinensis* Seed Shell Samples

No.	Retention Time (min)	Peak Area (%)	Component
1	3.70	0.07	2-Heptanol, 6-amino-2-methyl-
2	4.07	14.19	Ethyne, fluoro-
3	4.24	7.10	Carbon dioxide
4	4.36	1.59	Cyclobutanol
5	4.67	0.80	Acetone
6	4.70	1.93	Acetone
7	4.90	0.22	Acetic acid, methyl ester
8	5.17	0.13	1-Propene, 3-methoxy-
9	5.32	0.44	Acetaldehyde, hydroxy-
10	5.45	0.57	2,3-Butanedione
11	5.61	0.38	2-Butanone
12	5.68	1.75	Furan, 3-methyl-
13	6.07	6.26	Acetic acid
14	6.41	0.05	2-Butenal
15	6.45	0.10	Butanal, 3-methyl-
16	6.65	2.03	2-Propanone, 1-hydroxy-
17	6.82	0.10	3-Buten-2-one, 3-methyl-
18	7.10	0.09	2-Pentanone
19	7.21	0.08	2,3-Pentanedione
20	7.39	0.14	Furan, 2-ethyl-
21	7.54	0.52	Furan, 2,5-dimethyl-
22	7.73	0.39	Propanoic acid
23	7.93	0.05	3-Methylpyridazine
24	8.00	0.10	Propanoic acid, 2-oxo-, methyl ester
25	8.33	0.06	3-Penten-2-one, (E)-
26	8.39	0.12	1H-Pyrrole, 1-methyl-
27	8.62	0.15	Pyridine
28	8.74	0.46	Pyrrole
29	9.10	0.97	Toluene
30	9.27	0.09	2-Butenal, 2-methyl-, (E)-
31	9.44	0.16	Acetylacetone
32	9.62	0.31	Propanoic acid, 2-oxo-, methyl ester
33	9.76	0.10	Cyclopentanone
34	9.94	0.41	3-Amino-s-triazole
35	10.02	0.07	Furan, 2-ethyl-5-methyl-
36	10.39	0.06	3-Furaldehyde

No.	Retention Time (min)	Peak Area (%)	Component
37	10.46	0.05	Furan, 2-ethyl-5-methyl-
38	10.92	0.07	Propargylamine
39	11.02	0.67	Furfural
40	11.08	0.51	2-Cyclopenten-1-one
41	11.22	0.14	1H-Pyrrole, 3-methyl-
42	11.53	0.12	1H-Pyrrole, 2-methyl-
43	11.71	0.51	2-Furanmethanol
44	11.78	0.11	5,9-Dodecadien-2-one, 6,10-dimethyl-, (E,E))-
45	12.00	0.08	Ethylbenzene
46	12.09	0.37	2-Propanone, 1-(acetyloxy)-
47	12.19	0.09	2(3H)-Furanone, 5-methyl-
48	12.24	0.13	p-Xylene
49	12.70	0.10	Cyclopent-4-ene-1,3-dione
50	12.95	0.09	1,3,5,7-Cyclooctatetraene
51	13.05	0.05	Benzene, 1,3-dimethyl-
52	13.28	0.07	2-Butenoic acid, 2-methyl-, (Z)-
53	13.33	0.14	2-Butenoic acid, 2-methyl-
54	13.39	0.07	2-Butenoic acid, 2-methyl-, (Z)-
55	13.45	0.20	2-Cyclopenten-1-one, 2-methyl-
56	13.58	0.19	Ethanone, 1-(2-furanyl)-
57	13.70	0.63	2(5H)-Furanone
58	13.92	0.48	Heptane, 3-ethyl-4-methyl-
59	14.00	0.10	2-Propenoic acid, 3-(dimethylamino)-, methyl ester
60	14.09	0.75	2-Cyclopenten-1-one, 2-hydroxy-
61	14.37	0.20	2-Butenoic acid, 2-methyl-
62	14.49	0.19	2-Butenoic acid, 2-methyl-
63	14.52	0.07	2(5H)-Furanone, 5-methyl-
64	14.79	0.07	Methanamine, N-(1-methyl-2-pyrrolidinylidene)-
65	15.17	0.15	3-Pentanone, 2-methyl-
66	15.31	0.34	2-Furancarboxaldehyde, 5-methyl-
67	15.42	0.33	2-Cyclopenten-1-one, 3-methyl-
68	15.63	0.04	3-Fluoro-o-xylene
69	15.84	1.37	Phenol
70	15.94	0.04	Phenol
71	16.38	0.22	Mesitylene
72	16.50	0.26	2-Methyliminoperhydro-1,3-oxazine
73	16.58	0.14	2-Furanone, 2,5-dihydro-3,5-dimethyl
74	17.04	0.13	4(1H)-Pyrimidinone, 6-hydroxy-
75	17.37	0.04	o-Cymene

No.	Retention Time (min)	Peak Area (%)	Component
76	17.51	0.49	3-Methylcyclopentane-1,2-dione
77	17.88	0.16	2-Cyclopenten-1-one, 2,3-dimethyl-
78	18.03	0.08	4-Methyl-5H-furan-2-one
79	18.10	0.17	2,4-Imidazolidinedione, 5-methyl-
80	18.23	0.36	Phenol, 2-methyl-
81	18.56	0.02	Ethanone, 1-(1H-pyrrol-2-yl)-
82	18.62	0.06	Furaneol
83	18.74	0.07	Acetophenone
84	18.84	1.19	p-Cresol
85	19.01	0.08	2-Cyclopenten-1-one, 3-ethyl-
86	19.11	0.08	Ethanone, 1-cyclopentyl-
87	19.21	0.07	Methyl 2-furoate
88	19.28	0.12	2,5-Dimethylfuran-3,4(2H,5H)-dione
89	19.38	0.29	Phenol, 2-methoxy-
90	19.54	0.23	2-Formylhistamine
91	19.74	0.44	2-Formylhistamine
92	19.85	0.09	Benzofuran, 2-methyl-
93	19.98	0.07	Benzofuran, 2-methyl-
94	20.09	0.25	Maltol
95	20.26	0.23	Imidazole, 5-hydrazinocarbonyl-
96	20.28	0.29	4-Pyridinol
97	20.35	0.15	c-(3-Methyl-4,5-dihydroisoxazol-5-yl)methylamine
98	20.59	0.15	2-Pyrazoline-1-carboxaldehyde, 5-tert-butyl-5-hydroxy-3-methyl-
99	20.73	0.04	Benzyl nitrile
100	20.76	0.06	2(1H)-Pyridinone, 3-methyl-
101	20.86	0.13	Phenol, 3,5-dimethyl-
102	20.88	0.10	Phenol, 2,5-dimethyl-
103	21.07	0.12	Imidazoline, 1,3-dinitro-
104	21.28	0.10	Phenol, 4-ethyl-
105	21.34	0.20	Phenol, 3,5-dimethyl-
106	21.41	0.14	Thiazole, 4-propyl-
107	21.60	0.05	Phenol, 2,3-dimethyl-
108	21.69	0.11	D-erythro-Pentose, 2-deoxy-
109	21.71	0.20	1,3-Propanediol, 2-ethyl-2-(hydroxymethyl)-
110	21.85	0.15	Creosol
111	21.93	0.12	Phenol, 2-ethyl-
112	22.13	14.56	Catechol
113	22.26	0.16	Catechol
114	22.31	0.14	Catechol

No.	Retention Time (min)	Peak Area (%)	Component
115	22.38	0.19	Catechol
116	22.46	0.13	Benzofuran, 2,3-dihydro-
117	22.50	0.44	1,4:3,6-Dianhydro-.alpha.-d-glucopyranose
118	22.73	0.10	Catechol
119	22.85	0.44	2-Isopropoxyphenol
120	22.91	0.08	Phenyl-1-thio-.alpha.-d-glucofuranoside
121	22.96	0.14	2-Coumaranone
122	23.07	0.15	Isophthalaldehyde
123	23.15	0.06	1-Methoxybicyclo[2,2,2]oct-5-en-2-yl methyl ketone
124	23.31	0.10	2,3-Dimethylanisole
125	23.37	0.48	1,2-Benzenediol, 3-methyl-
126	23.44	0.14	Naphthalene, 2,7-bis(1,1-dimethylethyl)-
127	23.51	0.21	meta-Methoxybenzenethiol
128	23.58	0.14	N-[2-(2-Hydroxy-1-naphthylmethyleneamino)-4-methoxyphenyl]acetamide
129	23.78	0.33	Sulfide, isopropyl phenyl
130	23.82	0.28	Benzaldehyde,-2-ethoxy-5-methoxy
131	23.96	5.89	1,2-Benzenediol, 4-methyl-
132	24.12	0.37	Indolizine
133	24.29	0.37	2H-1-Benzopyran, 3,4-dihydro-
134	24.37	0.19	1,3-Benzenediol, 2-methyl-
135	24.44	0.43	2-Methoxy-4-vinylphenol
136	24.55	0.18	Benzene, [(2-methylpropyl)thio]-
137	24.75	0.51	Phenol, 3-isopropoxy-5-methyl-
138	24.85	0.16	(1S,3aR,4R,8R,8aS)-1-Isopropyl-3a-methyl-7-methylenedecahydro-4,8-epithioazulene
139	24.89	0.11	Benzaldehyde, 3,5-dimethyl-
140	24.96	0.32	Benzenemethanol, 3-hydroxy-
141	25.06	0.56	2,3-Dimethylhydroquinone
142	25.16	0.46	2H-Benzimidazol-2-one, 1,3-dihydro-, hydrazone
143	25.32	0.25	1H-1,3-Benzimidazole-2-methanol
144	25.47	0.23	2(equat)-Methyl-trans-decahydroquinol-4-one
145	25.56	0.74	2-(2-Methylcyclopropyl)thiophene
146	25.66	0.50	11-Bromoundecanoic acid
147	25.73	0.33	Indole, 3-methyl-
148	25.77	0.18	Ethanol, 2-(3,3-dimethylcyclohexylidene)-, (Z)-
149	25.95	0.74	3-Methylbenzothiophene
150	26.13	0.45	Pyrrole-2-carbonitrile, 5-formyl-3,4-dimethyl-
151	26.21	0.19	Myrtenoic acid, butyl ester
152	26.44	0.14	3-Pyridinecarbonitrile, 2-methoxy-4,6-dimethyl-

No.	Retention Time (min)	Peak Area (%)	Component
153	26.55	0.17	4-Hydroxyimino-4,5,6,7-tetrahydrobenzofurazan
154	26.64	0.21	3-Allyl-6-methoxyphenol
155	26.68	0.24	Cyclodecanone, oxime
156	26.80	0.22	2-Methyl-4-(methylthio)-2,3-dihydrothiophene
157	26.83	0.26	2-Methyl-4-(methylthio)-2,3-dihydrothiophene
158	26.91	0.28	4-Methoxyphenylglyoxal, aldoxime
159	27.19	0.10	Tetradecane, 1-bromo-
160	27.25	0.08	(S)-(-)-Citronellic acid, methyl ester
161	27.35	0.11	Benzene, 1-(2-methoxy-1-propenyl)-4-methyl-
162	27.67	3.81	D-Allose
163	27.80	0.16	11-Bromoundecanoic acid
164	27.84	0.15	Chloroacetic acid, 1-naphthyl ester
165	27.92	0.17	11-Bromoundecanoic acid
166	28.18	0.53	Dodecanoic acid
167	28.47	0.14	4-Methyl-2,5-dimethoxybenzaldehyde
168	28.70	0.09	[1,2,4]Triazolo[1,5-a]pyrimidin-5-ol, 7-methyl-6-nitro-
169	28.79	0.13	Isoxazole, 3,5-dimethyl-4-bromo-
170	28.98	0.07	1,4-Naphthalenedione, 5,8-dihydroxy-2,7-dimethoxy-
171	29.06	0.01	9-Hexadecenoic acid, tetradecyl ester, (Z)-
172	29.82	0.04	Silane, methylvinyl(2-methylphenoxy)isopropoxy-
173	29.85	0.04	Cyclodeca[b]furan-2(3H)-one, decahydro-6,10-dimethyl-3-methylene-
174	30.09	0.08	1,8-Naphthyridine, 2,7-dimethyl-
175	31.11	0.05	5-Isopropenyloxymethylene-3,3-dimethyl-cyclohexanone
176	31.58	0.11	5-Fluoro-2-(piperidin-4-yl)-1H-1,3-benzodiazole
177	31.73	0.30	[1,1'-Biphenyl]-2,2'-diol
178	32.12	0.17	Tetradecanoic acid
179	32.55	0.15	1H-phenalen-5-ol, 2,3,7,8,9,9a-hexahydro-
180	32.71	0.43	cis-9-Hexadecenal
181	33.09	0.09	5-Cyclohexadecen-1-one
182	33.73	0.09	Androstan-17-one, oxime, (5.alpha.)-
183	33.77	0.13	Ethyl 3-(3,4-dimethoxyphenyl)acrylate
184	34.48	0.00	E-11-Hexadecenal
185	35.35	0.11	Docosanoic acid
186	35.40	0.16	Octadecanoic acid
187	36.43	0.08	(1S,15S)-Bicyclo[13.1.0]hexadecan-2-one
188	36.47	0.02	Ethyl 3-(3,4-dimethoxyphenyl)acrylate
189	37.91	0.07	3-pentanone, 1,5-bis(4-hydroxy-2-methoxyphenyl)-
190	39.13	1.10	n-Hexadecanoic acid

No.	Retention Time (min)	Peak Area (%)	Component
191	39.23	0.09	Oleic Acid
192	39.63	0.14	Dibutyl phthalate